



Autosimilarité et anisotropie : applications en imagerie médicale

Hermine Biermé

journées MAS, Bordeaux, 03/09/2010

ANR-09-BLAN-0029-01 mataim [F. Richard (MAP5)] (www.mataim.fr)

Coll: INSERM U 658 [Pr. C.L. Benhamou (CHRO)], INSERM ERI-20 [Pr. F. Clavel (IGR)]

`hermine.bierme@mi.parisdescartes.fr`

Outlines

| | | |
|----------|---|-----------|
| 1 | Fractal analysis of medical images | 3 |
| 1.1 | Examples | 4 |
| 1.2 | Variogram method | 6 |
| 1.3 | Fractional Brownian motion modeling | 8 |
| 2 | Stochastic modeling for images | 14 |
| 2.1 | Restriction on a line | 15 |
| 2.2 | Fractional Brownian field | 16 |
| 2.3 | Anisotropic Gaussian field | 19 |
| 2.4 | Validation for bone radiographs | 23 |

1 Fractal analysis of medical images

ROI medical images = textures

Goal: use texture analysis to extract diagnostically meaningful information

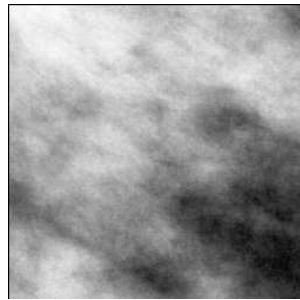
One tool: fractal analysis to characterize texture via statistical self-similarity or scale invariance through a fractal index $H \in (0, 1)$

Numerous methods and studies!

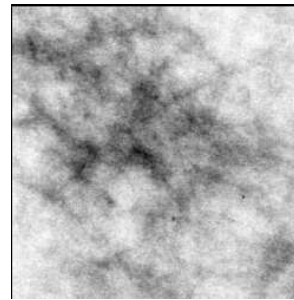
[Lopes and Betrouni, 2009]

1.1 Examples

Mammography



dense breast tissue

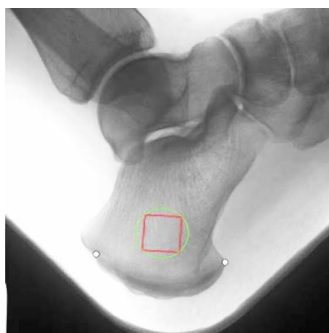


fatty breast tissue

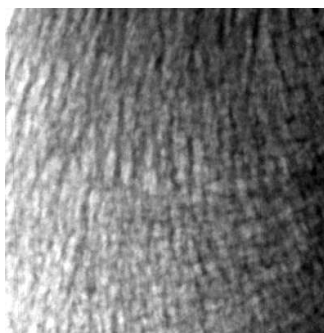
- Validation of self-similarity using power spectrum method $H \in [0.33, 0.42]$ [Heine et al, 2002].
- Discrimination of dense $H \in [0.55, 0.75]$ and fatty $H \in [0.2, 0.35]$ breast tissue using WTMM method [Kestener et al, 2001]

Trabecular bone microarchitecture

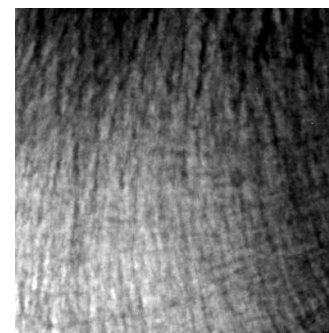
Dataset of 211 high-resolution digital X-ray images of calcaneum (a heel bone) with standardized acquisition procedure [Lespessailles et al., 2007]:



ROI location



control case



osteoporotic case

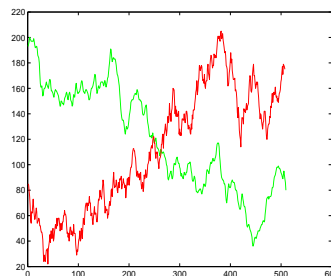
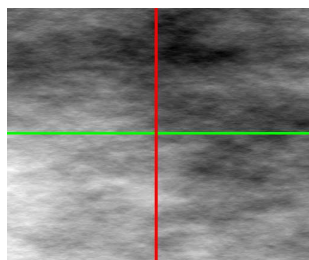
- Validation of self-similarity using variogram and power spectrum methods on calcaneous bone [Benhamou et al, 94], on cancellous bone [Caldwell et al, 94]
- Discrimination of osteoporotic cases $H_{mean} = 0.679 \pm 0.053$ (osteoporotic cases) / $H_{mean} = 0.696 \pm 0.030$ (control cases) [Benhamou et al, 2001]

1.2 Variogram method

Let us consider the discrete image

$$I(k, l), 0 \leq k \leq n - 1, 0 \leq l \leq n - 1.$$

Extract a line of the image $I_\theta(k), 0 \leq k \leq n_\theta - 1$ for θ a direction.

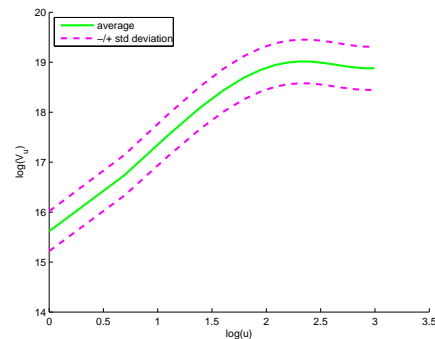


Compute
$$v_\theta(u) = \frac{1}{n_\theta - u} \sum_{k=0}^{n_\theta - 1 - u} (I_\theta(k + u) - I_\theta(k))^2, 1 \leq u \leq n_\theta - 1.$$

Average along a set of lines with the same direction $\bar{v}_\theta(u)$ and plot $\log \bar{v}_\theta(u)$ versus $\log(u)$.

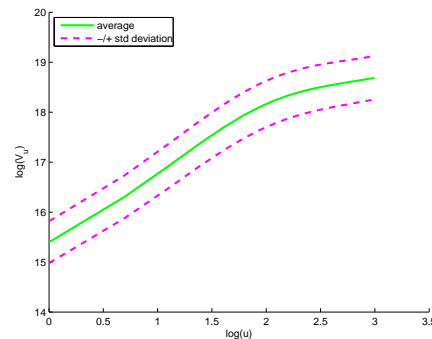
➔ Fractal index $H_\theta = \text{slope}(\theta)/2$

Example on bone radiographs (211 cases):



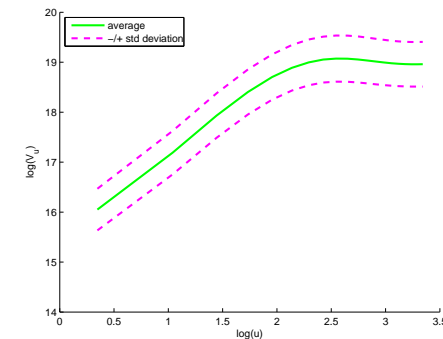
$\theta = (1, 0)$ (horizontal)

$$H_\theta = 0.51 \pm 0.08$$



$\theta = (0, 1)$ (vertical)

$$H_\theta = 0.56 \pm 0.06$$



$\theta = (1, 1)/\sqrt{2}$ (diagonal)

$$H_\theta = 0.51 \pm 0.08$$

1.3 Fractional Brownian motion modeling

Let $(\Omega, \mathcal{A}, \mathbb{P})$ be a probability space. For $H \in (0, 1)$, the fractional Brownian motion [Kolmogorov, 1940], [Mandelbrot and Van Ness, 1968] $B_H = \{B_H(t); t \in \mathbb{R}\}$ is a zero mean Gaussian random process such that

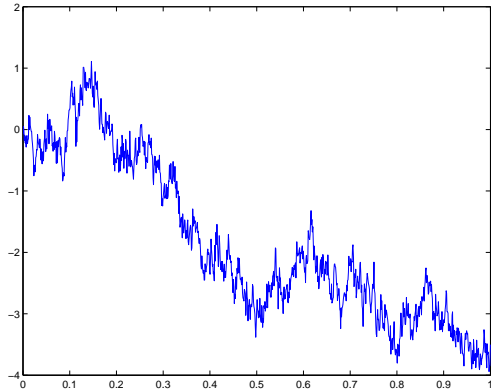
$$\forall t \in \mathbb{R}, B_H(t) : \Omega \rightarrow \mathbb{R} \text{ real random variable } \sim \mathcal{N}\left(0, |t|^{2H}\right).$$

and

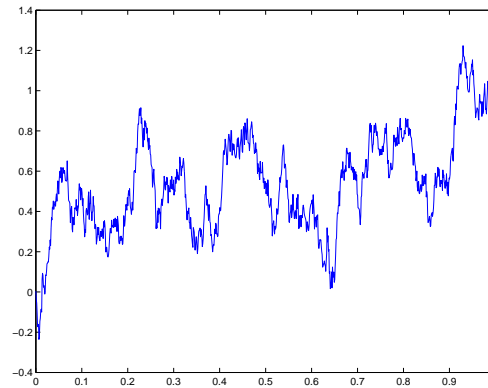
$$\text{Cov}(B_H(t), B_H(s)) = \frac{1}{2} \left(|t|^{2H} + |s|^{2H} - |t - s|^{2H} \right).$$

Properties :

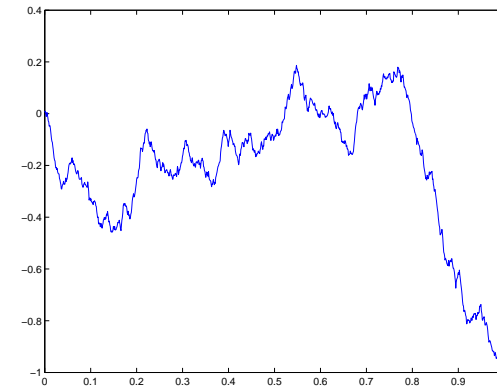
- $B_H(0) = 0$ a.s.
- Stationary increments: $\forall t_0 \in \mathbb{R}, B_H(\cdot + t_0) - B_H(t_0) \stackrel{fdd}{=} B_H(\cdot)$
- Self-similarity of order H : $\forall \lambda > 0, B_H(\lambda \cdot) \stackrel{fdd}{=} \lambda^H B_H(\cdot)$.



$H = 0.3$



$H = 0.5$



$H = 0.7$

- $H =$ Self-similarity/Hölder regularity/Fractal dimension : $2 - H$
 - ↳ Numerous estimators of H .
- Law characterized by the variogram $v_H(t) = \text{Var}(B_H(t)) = |t|^{2H}$.
- Spectral representation $B_H(t) = c_H \int_{\mathbb{R}} (e^{-it\xi} - 1) |\xi|^{-H-1/2} dW(\xi)$

$$v_H(t) = c_H^2 \int_{\mathbb{R}} |e^{-it\xi} - 1|^2 |\xi|^{-2H-1} d\xi$$
 - ↳ spectral density = $c_H^2 |\xi|^{-2H-1}$ [1/f process].

Estimation

Let us observe $\{I_\theta(k) = c_\theta B_H \left(\frac{k}{n}\right); 0 \leq k \leq n-1\}$.

$$V_{1,u}(B_H) := \frac{c_\theta^2}{n-u} \sum_{k=0}^{n-1-u} \left(B_H \left(\frac{k+u}{n} \right) - B_H \left(\frac{k}{n} \right) \right)^2$$

$$\rightarrow \mathbb{E}(V_{1,u}(B_H)) = \frac{c_\theta^2}{n-u} \sum_{k=0}^{n-1-u} v_H \left(\frac{u}{n} \right) = c_\theta^2 n^{-2H} u^{2H}.$$

Ergodic Theorem: $V_{1,u}(B_H) / \mathbb{E}(V_{1,u}(B_H)) \xrightarrow[n \rightarrow +\infty]{} 1$ a.s.

$$\hat{H} = \frac{1}{2} \log \left(\frac{V_{1,u}(B_H)}{V_{1,v}(B_H)} \right) / \log \left(\frac{u}{v} \right)$$

Remark:

$$v_H \left(\frac{u}{n} \right) = \text{variogram at small scales} = \begin{cases} -\text{H\"older regularity} \\ -\text{spectral density at high frequencies} \end{cases}$$

Rate of convergence: asymptotic normality?

$$P^K(x) = (1-x)^K = \sum_{l=0}^K a_l x^l \text{ filter of order } K \geq 1$$

$$\begin{aligned} \forall t \in \mathbb{R}, P_u^K(B_H)(t) &= \sum_{l=0}^K a_l B_H\left(\frac{t+lu}{n}\right) \\ &= c_H \int_{\mathbb{R}} e^{-i\frac{t\xi}{n}} P\left(e^{-i\frac{u\xi}{n}}\right)^K |\xi|^{-H-\frac{1}{2}} dW(\xi) \end{aligned}$$

→ stationary ergodic Gaussian process

Generalized quadratic variations [Istas and Lang, 1997]

$$V_{K,u}(B_H) = \frac{1}{n-Ku} \sum_{k=0}^{n-Ku+1} (P_u^K(B_H)(k))^2 \text{ with ,}$$

$$\mathbb{E}(V_{K,u}(B_H)) = c_{K,H} n^{-2H} u^{2H}.$$

Ergodic Theorem: $V_{K,u}(B_H) / \mathbb{E}(V_{K,u}(B_H)) \xrightarrow[n \rightarrow +\infty]{} 1$ a.s.

$$\sqrt{n - Ku} \left(\frac{V_{K,u}(B_H)}{\mathbb{E}(V_{K,u}(B_H))} - 1 \right) \stackrel{fdd}{=} \frac{1}{\sqrt{n - Ku}} \sum_{k=0}^{n-Ku-1} H_2(X_u)(k),$$

with $H_2(x) = x^2 - 1 = 2\text{th-Hermite polynomial}$ and X_u is a centered stationary Gaussian time series which admits for spectral density

$$F_{X_u}(\xi) = \frac{2\pi}{c_{K,H}u^{2H}} \left| P(e^{-iu\xi}) \right|^{2K} \sum_{k \in \mathbb{Z}} |\xi + 2k\pi|^{-2H-1},$$

ie

$$\text{Cov}(X_u(k + k'), X_u(k')) = \frac{1}{2\pi} \int_{-\pi}^{+\pi} e^{-ik\xi} F_{X_u}(\xi) dx.$$

Theorem:[Breuer-Major, 1983] If $\int_{\mathbb{R}} |P(e^{-iu\xi})|^{4K} |\xi|^{-4H-2} d\xi < +\infty$, then, $F_{X_u} \in L^2([-\pi, \pi])$ and, as $n \rightarrow +\infty$,

$$\sqrt{n - Ku} \left(\frac{V_{K,u}(B_H)}{\mathbb{E}(V_{K,u}(B_H))} - 1 \right) \rightarrow \mathcal{N}(0, \sigma_u^2)$$

with $\sigma_u^2 = 2F_{X_u}^{*2}(0)$.

New proof by [Nualart, Ortiz-Latorre, 2008], [Nourdin, Peccatti, 2009]
 + **vectorial CLT** from [Peccatti, Tudor, 2004]

Theorem:[B., Bonami and León, 2010]

Let $Y(t) = \int_{\mathbb{R}} (e^{-it\xi} - 1) f(\xi)^{1/2} dW(\xi)$, with

$$f(\xi) = \frac{c}{|\xi|^{2H+1}} + o_{|\xi| \rightarrow +\infty} \left(\frac{1}{|\xi|^{2H+1+\gamma}} \right),$$

Then, $\hat{H} = \frac{1}{2} \log \left(\frac{V_{K,u}(Y)}{V_{K,v}(Y)} \right) / \log \left(\frac{u}{v} \right) \xrightarrow{n \rightarrow +\infty} H$ a.s.

+ asymptotic normality for $K > H + 1/4$ and $\gamma > 1/2$.

2 Stochastic modeling for images

$\{X(x); x \in \mathbb{R}^2\}$ a zero mean Gaussian random field

Spectral representation: [Bonami and Estrade, 2003]

$$X(x) = \int_{\mathbb{R}^2} \left(e^{-ix \cdot \xi} - 1 \right) f(\xi)^{1/2} dW(\xi), x \in \mathbb{R}^2$$

well defined for $f \geq 0$ even and $\int_{\mathbb{R}^2} \min(1, \|\xi\|^2) f(\xi) d\xi < +\infty$.

Properties :

- $X(\mathbf{0}) = 0$ a.s.
- Stationary increments: $\forall x_0 \in \mathbb{R}^2, X(\cdot + x_0) - X(x_0) \stackrel{fdd}{=} X(\cdot)$
- $\text{Cov}(X(x), X(y)) = \frac{1}{2} (v_X(x) + v_X(y) - v_X(x - y))$ with

$$v_X(x) = \int_{\mathbb{R}^2} \left| e^{-ix \cdot \xi} - 1 \right|^2 f(\xi) d\xi$$

↪ f spectral density

2.1 Restriction on a line

For all direction $\theta \in S^1$, $\{X(t\theta); t \in \mathbb{R}\}$ is a zero mean Gaussian random process with spectral density given by

$$R_\theta f(\tau) = \int_{\mathbb{R}} f(\tau\theta + \gamma\theta^\perp) d\gamma \text{ a.e. } \tau \in \mathbb{R}$$

Self-similarity: $R_\theta f(\tau) = c_\theta |\tau|^{-2H-1}$

$$f(\xi) = c(\arg(\xi)) \|\xi\|^{-2H-2}, \text{ a.e. } \xi \in \mathbb{R}^2$$

$$\forall \lambda > 0, X(\lambda \cdot) \stackrel{fdd}{=} \lambda^H X(\cdot).$$

Isotropy: $R_{\theta'} f = R_\theta f$ for all $\theta' \in S^1$

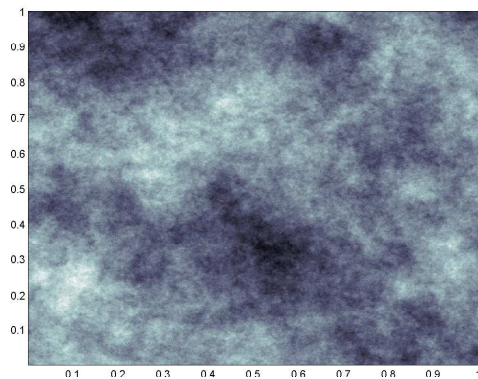
f is radial

$$\forall M \in \mathcal{O}_2(\mathbb{R}), X(M \cdot) \stackrel{fdd}{=} X(\cdot).$$

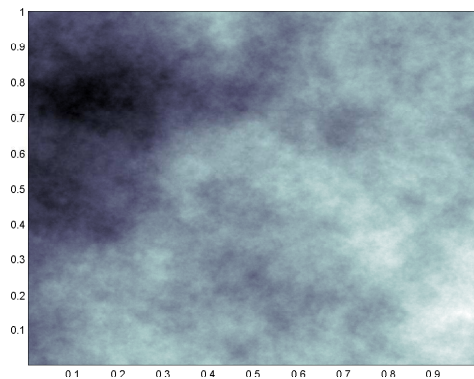
2.2 Fractional Brownian field

$$f(\xi) = c_H \|\xi\|^{-2H-2} \text{ a.e. } \xi \in \mathbb{R}^2 \text{ and } \forall x \in \mathbb{R}^2, v_X(x) = \text{Var}(X(x)) = \|x\|^{2H}.$$

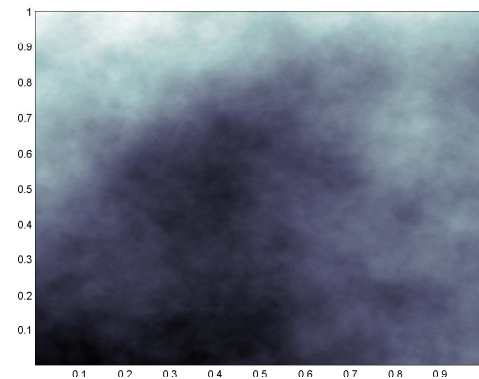
Exact method of simulation [Stein, 2002]



$$H = 0.3$$

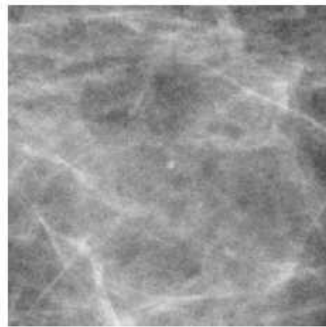


$$H = 0.5$$

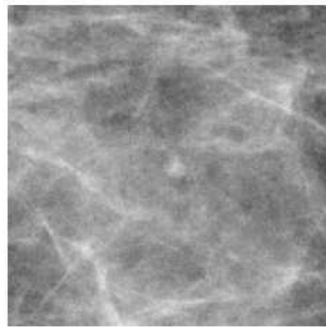


$$H = 0.7$$

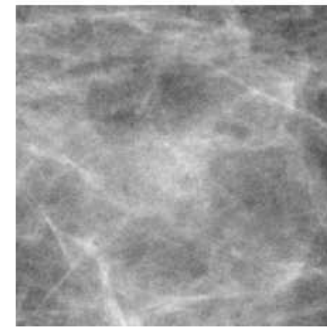
Detectability of spots on mammograms [Grosjean, Moisan, 2009]



radius 5



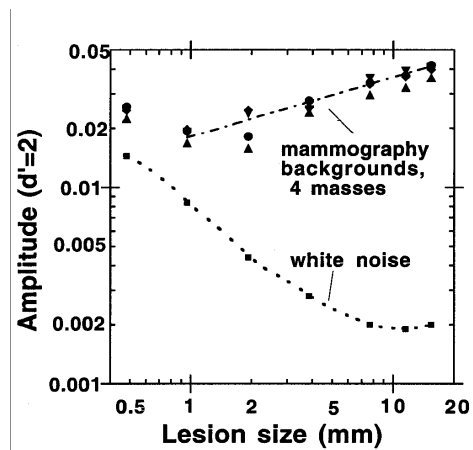
radius 10



radius 50

Simulated spots with identical contrast on a real mammogram

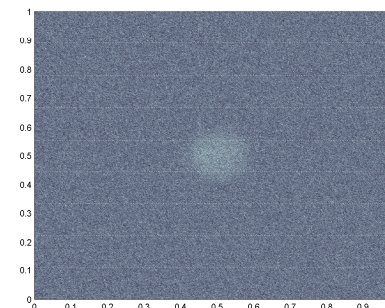
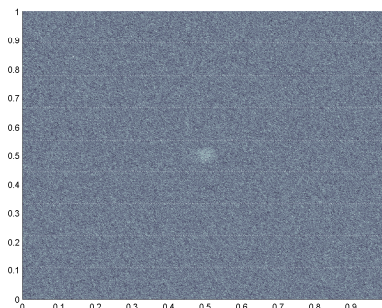
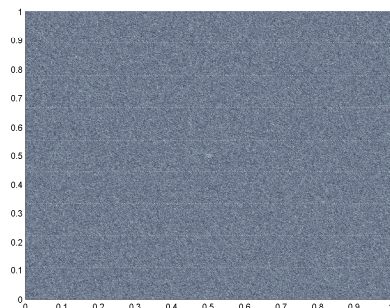
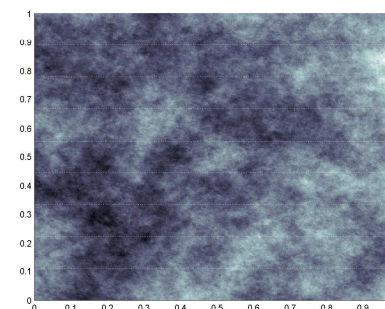
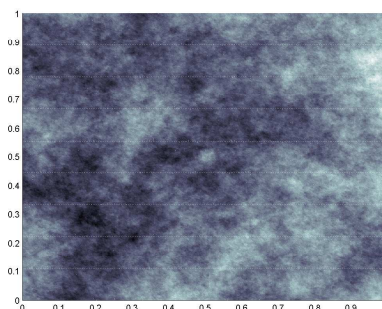
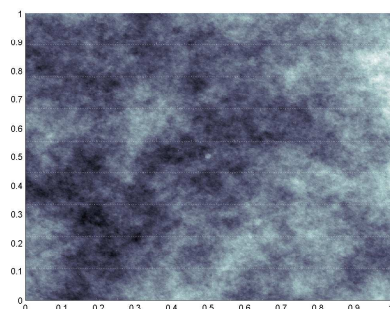
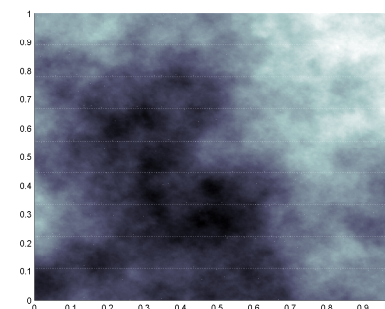
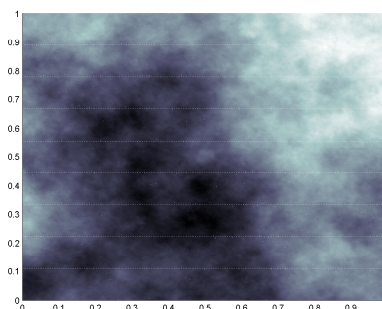
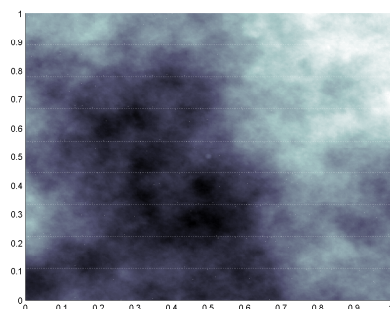
Burgess' Law [Burgess et al, 2001]



Link between size and contrast for human perception of opacities and mammograms

Simulated spots with identical contrast

WN

 $H = 0.3$  $H = 0.7$ 

radius 5

radius 10

radius 50

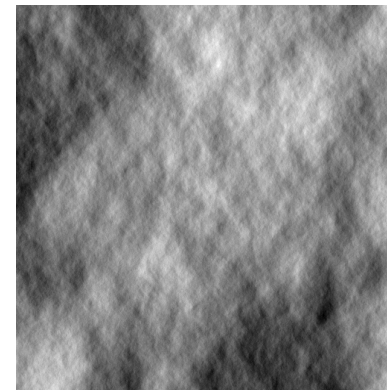
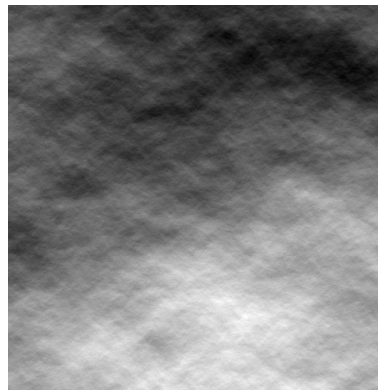
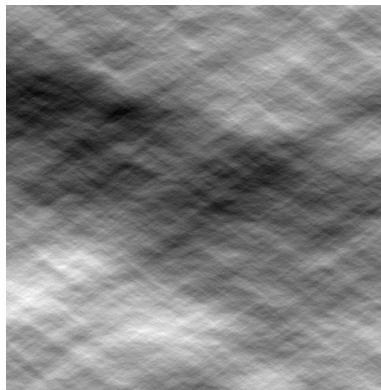
2.3 Anisotropic Gaussian field

$$f(\xi) = c(\arg(\xi)) \|\xi\|^{-2H-2} \text{ a.e. } \xi \in \mathbb{R}^2$$

$$\forall x \in \mathbb{R}^2, v_X(x) = \text{Var}(X(x)) = C(\arg(x)) \|x\|^{2H}.$$

C = topothesy function [Davies and Hall, 1999] with $\forall \theta, C(\theta) > 0$

Simulations for $H = 0.4$ [Coll: Moisan, Richard (MAP5)]



$$c(\theta) = \mathbf{1}_{[\pi/4, 3\pi/4]}(|\theta|)$$

$$c(\theta) = |\sin(\theta)|$$

$$c(\theta) = |\cos(\theta)|$$

- Identification of c [Istas, 2007]
- Anisotropy test for C [Coll: Bonami, León, Richard]

Anisotropic self-similarity?

Problem: Let $\theta_1 = (1, 0)$ and $\theta_2 = (0, 1)$. Find X such that

- $\{X(t\theta_1); t \in \mathbb{R}\}$ =FBM of order H_1
- $\{X(t\theta_2); t \in \mathbb{R}\}$ =FBM of order H_2 with $H_1 < H_2$

Remark: It is not possible to get more than 2 different directions due to S.I.

Toy example solution:

$X(x) = X(x_1, x_2) = B_{H_1}(x_1) + B_{H_2}(x_2)$ with B_{H_1} and B_{H_2} ind. FBMs.

Then

$$v_X(x) = |x_1|^{2H_1} + |x_2|^{2H_2} \rightarrow \text{no spectral density.}$$

Note that

$$\forall \lambda > 0, \quad v_X(\lambda x_1, \lambda^a x_2) = \lambda^{2H_1} v_X(x_1, x_2) \text{ with } a = H_1/H_2.$$

Operator scaling property

For $a = H_1/H_2$, $\forall \lambda > 0$,

$$\{X(\lambda x_1, \lambda^a x_2); (x_1, x_2) \in \mathbb{R}^2\} \stackrel{fdd}{=} \lambda^{H_1} \{X(x_1, x_2); (x_1, x_2) \in \mathbb{R}^2\}$$

A solution with spectral density f :

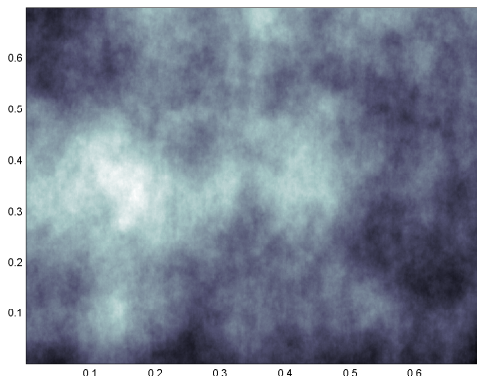
$$f(\lambda \xi_1, \lambda^a \xi_2) = \lambda^{-\beta} f(\xi_1, \xi_2), \quad \beta = 2H_1 + 1 + a$$

One example: $f(\xi_1, \xi_2) = (\xi_1^2 + \xi_2^{2a})^{-\beta/2}$

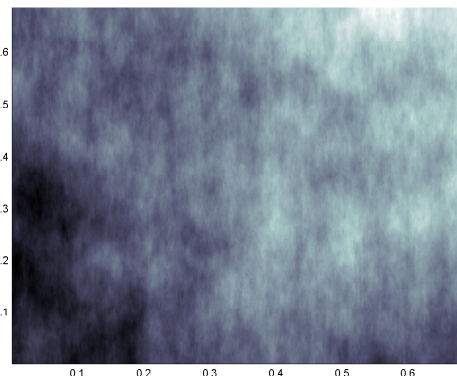
Theorem:[B., Meerschaert, Scheffler, 2007]: X is well defined and satisfies the operator scaling property

$$\forall \lambda > 0, X(\lambda^E \cdot) \stackrel{fdd}{=} \lambda^{H_1} X(\cdot), \quad \text{with } E = \begin{pmatrix} 1 & 0 \\ 0 & a \end{pmatrix}$$

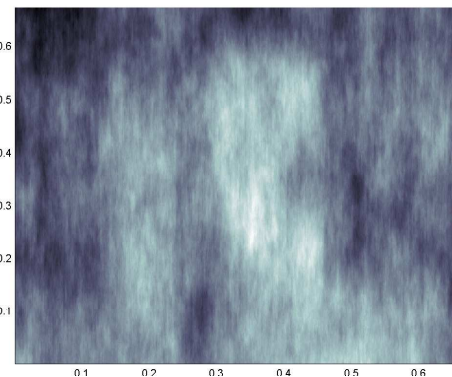
Simulations for $H_2 = 0.6$



$$H_1 = 0.55$$



$$H_1 = 0.5$$



$$H_1 = 0.45$$

What for other directions?

If $\theta = (\theta_1, \theta_2) \in S^1$ with $\theta_1 \neq 0$ and $\theta_2 \neq 0$,

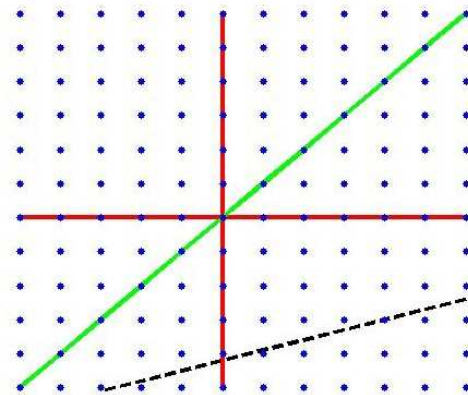
$$R_\theta f(p) \underset{+\infty}{\asymp} c_\theta |p|^{-2H_1-1} \text{ with } c_\theta = \frac{1}{|\theta_1|} \int_{\mathbb{R}} (s^{2a} + \theta_1^{-2})^{-\beta/2} ds$$

$$\rightarrow v_\theta(t) = \text{Var}(X(t\theta)) \underset{0}{\asymp} d_\theta |t|^{2H_1} \text{ with } d_\theta > 0.$$

2.4 Validation for bone radiographs

[Benhamou, B., Richard, 2009]

Implementation issues



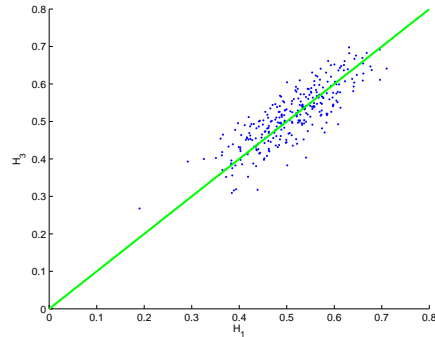
Black = out of lattice.

Precision of

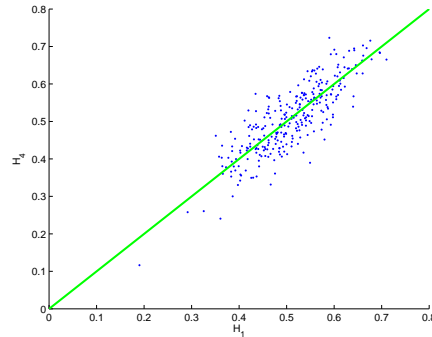
red = 1, green = $\sqrt{2}$

- Estimation on oriented lines **without interpolation**.
- Precision is not the same in all directions.
- Accuracy of orientation analysis \leftrightarrow Precision of the image.

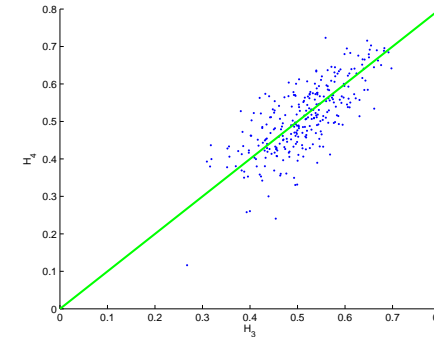
Comparison of the index in different directions



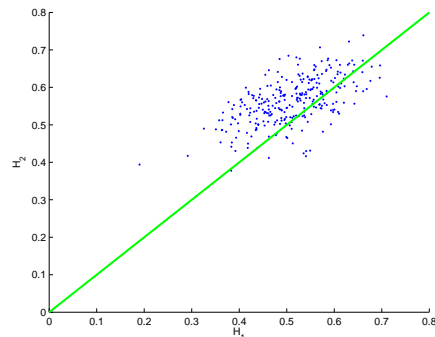
H_{θ_3} vs H_{θ_1}



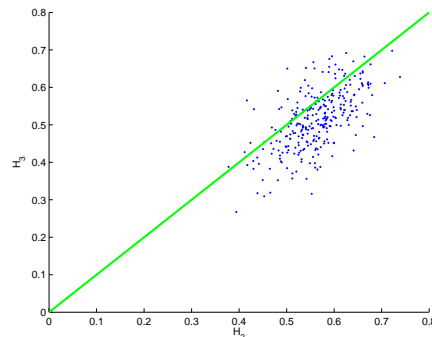
H_{θ_4} vs H_{θ_1}



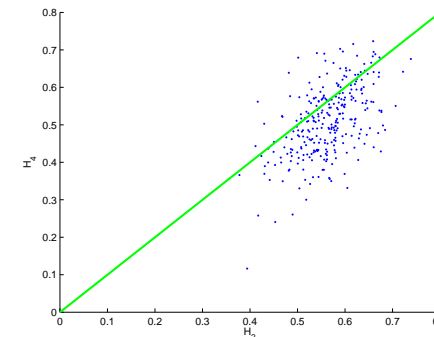
H_{θ_4} vs H_{θ_3}



H_{θ_3} vs H_{θ_2}



H_{θ_4} vs H_{θ_2}



H_{θ_4} vs H_{θ_1}

Directions:

1: $\theta_1 = (1, 0)$ (horizontal), 2: $\theta_2 = (0, 1)$ (vertical),

3: $\theta_3 = (1, 1)/\sqrt{2}$ (diagonal), 4: $\theta_4 = (-1, 1)/\sqrt{2}$ (diagonal).